A transgenic mouse model for the study of enterovirus 71 neuropathogenesis

Ken Fujii[a], Noriyo Nagata[c], Yuko Sato[c], Kien Chai Ong[d], Kum Thong Wong[e], Seiya Yamayoshi[a], Midori Shimanuki[b], Hiroshi Shitara[b], Choji Taya[b], and Satoshi Koike[a, 1].

[a]Neurovirology Project and [b]Laboratory for Transgenic Technology, Tokyo Metropolitan Institute of Medical Science, 2-1-6, Kamikitazawa, Setagaya-ku, Tokyo 156-8506, Japan [c]Department of Pathology, National Institute of Infectious Diseases, 4-7-1 Gakuen, Musashimurayama-shi, Tokyo 208-0011, Japan [d]Department of Biomedical Science and [e]Department of Pathology, Faculty of Medicine, University of Malaya, 50603 Kuala Lumpur, Malaysia

Submitted to Proceedings of the National Academy of Sciences of the United States of America

Enterovirus 71 (EV71) typically causes mild hand-foot-and-mouth disease in children, but it can also cause severe neurological disease. Recently, epidemic outbreaks of EV71 with significant mortality have been reported in the Asia-Pacific region, and EV71 infection has become a serious public health concern worldwide. However, there is little information available concerning EV71 neuropathogenesis, and no vaccines or anti-EV71 drugs have been developed. Previous studies of this disease have used monkeys and neonatal mice that are susceptible to some EV71 strains as models. The monkey model is problematic for ethical and economical reasons, and mice that are more than a few weeks old lose their susceptibility to EV71. Thus, the development of an appropriate small animal model would greatly contribute to the study of this disease. Mice lack EV71 susceptibility due to the absence of a receptor for this virus. Previously, we identified the human scavenger receptor class B, member 2 (hSCARB2) as a cellular receptor for EV71. In the current study, we generated a transgenic (Tg) mouse expressing hSCARB2 with an expression profile similar to that in humans. Tg mice infected with EV71 exhibited ataxia, paralysis and death. The most severely affected cells were neurons in the spinal cord, brainstem, cerebellum, hypothalamus, thalamus and cerebrum. The pathological features in these Tg mice were generally similar to those of EV71 encephalomyelitis in humans and experimentally infected monkeys. These results suggest that this Tg mouse could represent a useful animal model for the study of EV71 infection.

Enterovirus 71 | Mouse model | Neuropathologenesis

INTRODUCTION

Enterovirus 71 (EV71) is a human enterovirus species A of the genus *Enterovirus* within the *Picornaviridae* family, and it is known to be one of the causative agents of hand-foot-and-mouth disease (HFMD) (1, 2). HFMD is generally considered to be a mild exanthematous disease. However, in some infants and young children, after a few days of prodromal illness, HFMD caused predominantly by EV71, can be complicated by neurological manifestations, including ataxia, tremor, myoclonus, polio-like paralysis, encephalomyelitis, cardiopulmonary failure and death (3, 4). In humans with fatal EV71 encephalomyelitis, inflammation and viral antigens in neurons were observed mainly in the spinal cord, brainstem, hypothalamus, cerebellar dentate nucleus and cerebrum (5, 6). Since the 1970s, HFMD outbreaks with significant mortality have been reported throughout the world, including in Bulgaria in 1975 (44 deaths (7)), Hungary in 1978 (47 deaths (8)), Malaysia in 1997 (29 deaths (9)), Taiwan in 1998 (78 deaths (3)), China in 2008-2011 (1,894 deaths (10), (http://www.wpro.who.int/china/mediacentre/factsheets/hfmd/en/)), Vietnam in 2011 (166 deaths (http://www.wpro.who.int/emerging_diseases/HFMD/en/index.html)) and Cambodia in 2012 (http://www.wpro.who.int/mediacentre/releases/2012/20120713/en/index.html). Thus, EV71 infection has the potential to become the most serious public health issue caused by neurotropic picornaviruses after the eradication of poliovirus (PV). Unfortunately, there is still very little information concerning EV71 neuropathogenesis, and vaccines or anti-EV71 drugs have yet to be developed.

Appropriate animal models are needed to better understand EV71 neuropathogenesis and to facilitate the development of effective vaccines and drugs. EV71-infected cynomolgus monkeys developed neurological complications similar to those observed in human cases, including ataxia, tremor and flaccid paralysis (11-15), and pathological lesions were observed in the spinal cord, brainstem, cerebellar dentate nucleus and other parts of the brain (14, 15). However, the use of monkeys to model EV71 infection is difficult for both ethical and economical reasons. Other investigators have developed neonatal mouse models of EV71 infection using mouse-adapted virus strains or mice deficient in interferon receptors (16-20). Unfortunately, EV71 infection in neonatal mice is significantly different from that in humans, as the major viral replication sites in the mouse include the muscle and adipose tissues, which are not featured in human infection. Moreover, mice that are more than a few weeks old are generally not susceptible to EV71. Thus, it is necessary to establish a new experimental animal model that can overcome these limitations.

Viral receptors determine the host range specificity for certain enteroviruses (21). The transgenic (Tg) expression of the human poliovirus receptor (PVR), CD155, and the major group human rhinovirus receptor, intracellular adhesion molecule-1 (ICAM-1) in mice conferred susceptibility to PV and major group human rhinoviruses, respectively (22-24). These Tg mice are therefore good small animal models to study the pathogenesis of these viruses. Recently, sialylated glycans (25), annexin II (26), human P-selectin glycoprotein ligand-1 (PSGL-1) (27) and human scavenger receptor class B, member 2 (hSCARB2)

Significance

EV71 infection with severe neurological diseases has been becoming a serious public health concern. However, suitable animal models that mimic human EV71 pathogenesis were not available. By expressing human EV71 receptor, Scavenger receptor B2, in mice, we generated a Tg mouse model susceptible to EV71 and the mice infected with EV71 exhibited neurological diseases similar to those observed in human patients. The development of the new small animal model will greatly contribute to studies of EV71 pathogenesis and development of vaccines and anti-EV71 drugs.

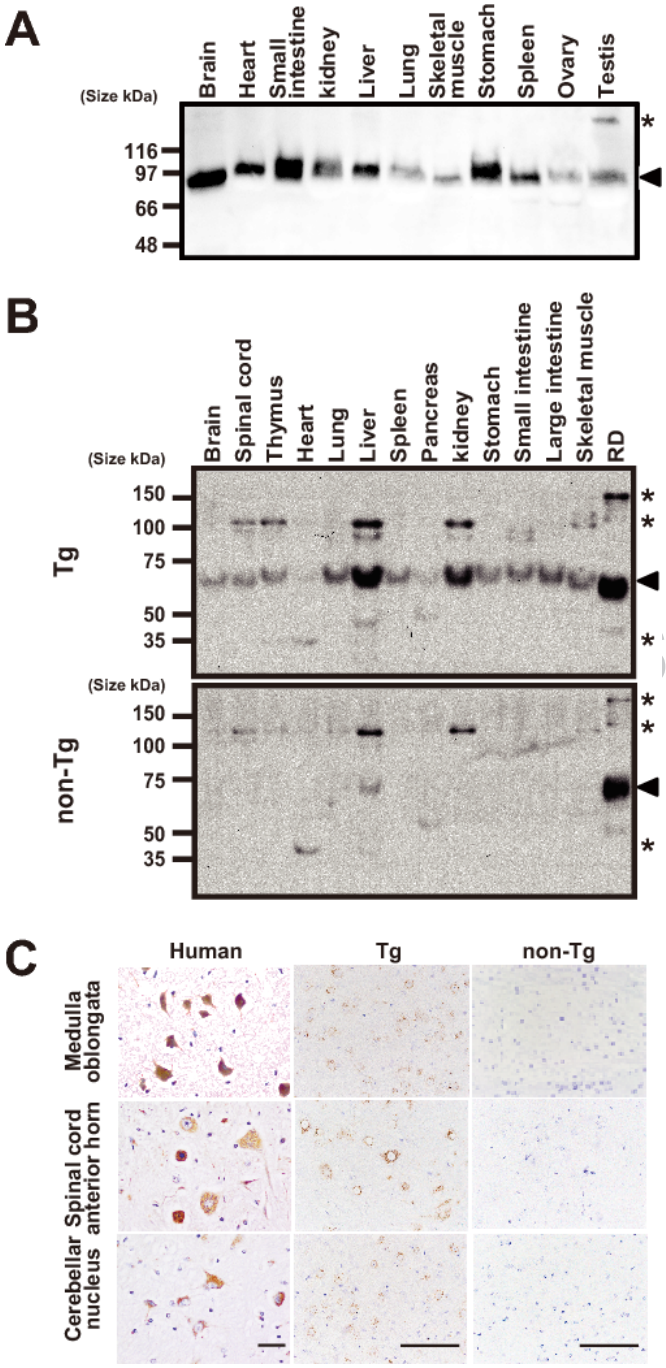

Fig. 1. Expression profiles of hSCARB2 in human and hSCARB2-Tg10 mouse tissues.

(28) were reported as candidate receptors for EV71. SCARB2, also known as lysosomal integral membrane protein-2, localizes mainly to lysosomes (29) and acts as a receptor for lysosomal targeting of β-glucocerebrosidase (30). Mouse cells transformed with hSCARB2 are rendered susceptible to all EV71 strains (31, 32), facilitating virus binding, internalization and uncoating (33), whereas mouse Scarb2 does not function as a receptor for EV71. Importantly, SCARB2 is widely expressed in many human tissues and cell types, including neurons in the central nervous system (CNS) (34-36). Moreover, there is no evidence that other candidates can support viral infection as efficiently as SCARB2. Transgenic expression of human PSGL-1 in mice was not sufficient to permit EV71 infection (37). Together, these

Table 1. Incidence of neurological signs in mice after EV71 inoculation

Inoculation route	mouse	Viral inoculation dose (Log_{10} $TCID_{50}$/animal)							
		1	2	3	4	5	6	7	8
ic	non-Tg	-	-	-	-	-	0/18*	-	-
	Tg	0/18	2/18	13/18	11/18	17/18	18/18	-	-
iv	non-Tg	-	-	-	-	-	0/18	-	-
	Tg	0/18	7/18	4/18	4/18	4/18	16/18	-	-
ip	non-Tg	-	-	-	-	-	0/18	-	-
	Tg	-	0/18	2/18	2/18	5/18	7/18	-	-
ig	non-Tg	-	-	-	-	-	-	-	0/10
	Tg	-	-	-	-	-	1/20	1/20	0 /10

Three-week-old mice were inoculated intracerebrally (ic), intravenously (iv), intraperitoneally (ip) or intragastrically (ig) with the EV71 Isehara strain at the indicated dose. After viral inoculation, the mice were observed daily for 2 weeks. *: Number of mice showing ataxia, paralysis and death/total number of inoculated mice; -, not performed.

Table 2. Incidence of neurological signs in Tg mice after intracerebral inoculation with EV71 and CVA16

Virus	Strain	Viral inoculation dose (Log_{10} $TCID_{50}$/animal)				
		2	3	4	5	6
EV71	Isehara*	2/18**	13/18	11/18	17/18	18/18
	BrCr	0/10	0/10	0/10	0/10	4/10
	SK-EV006	0/10	2/10	3/10	3/10	3/10
	C7	0/10	0/10	2/10	7/10	5/10
CVA16	G-10	0/10	0/10	1/10	1/10	2/10

Three-week-old mice were inoculated intracerebrally with one of four EV71 strains or the CVA16 G-10 strain at the indicated dose. After viral inoculation, the mice were observed daily for 2 weeks. *: The results shown for mice infected with the Isehara strain are indicted same results in Table 1. **: Number of mice showing ataxia, paralysis or death/total number of inoculated mice.

observations suggest that the expression of hSCARB2 in mice may confer susceptibility to EV71 infection. Here, we describe the generation and characterization of a Tg mouse expressing hSCARB2 and demonstrate its utility as a small animal model for the study of EV71 pathogenesis.

RESULTS

Generation of hSCARB2-Tg mice

To generate Tg mice expressing hSCARB2, two bacterial artificial chromosome (BAC) clones (RP11-54D17 and RP11-628A4) containing the complete *hSCARB2* gene and endogenous promoter were used (Fig. S1A). Genomic DNA was isolated from the resulting transgenic mice and subjected to PCR genotyping using the four primer sets indicated in Fig. S1B and Table S1. Four founder mice (C57BL/6 Tg(hSCARB2)10, 16, 22 and 24) and two founder mice (C57BL/6 Tg(hSCARB2)49 and 75) were obtained from the RP11-54D17-injected and RP11-628A4-injected groups, respectively. Using each primer set, the expected PCR product was amplified from Tg mice and positive control human rhabdomyosarcoma (RD) cells, but not from non-Tg mice (Fig. S1B). These results indicated that the Tg mice carried the entire *hSCARB2* gene in their genome. The analysis of the hemizygous C57BL/6 Tg(hSCARB2)10 mouse, which we refer to as hSCARB2-Tg10, is presented in this article. Similar results were also obtained using hemizygous hSCARB2-Tg16, 22 and 49 mice.

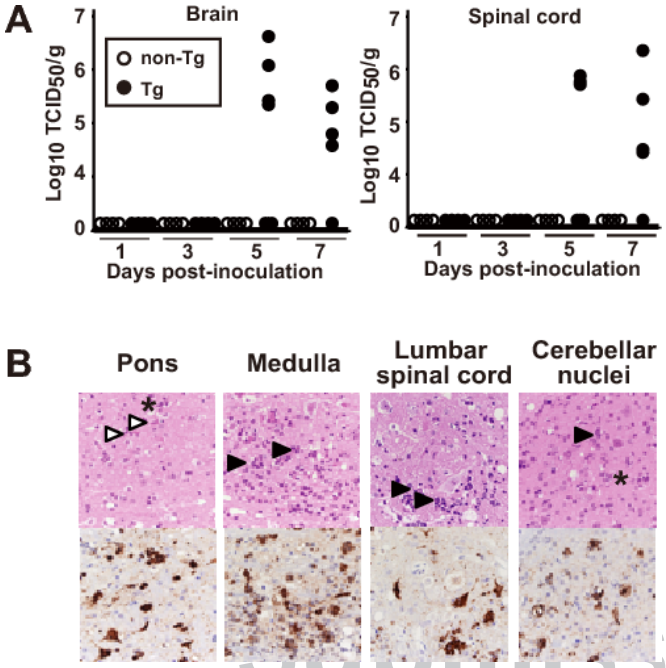

Fig. 2. Replication of EV71 in the CNS of hSCARB2-Tg10 mice.

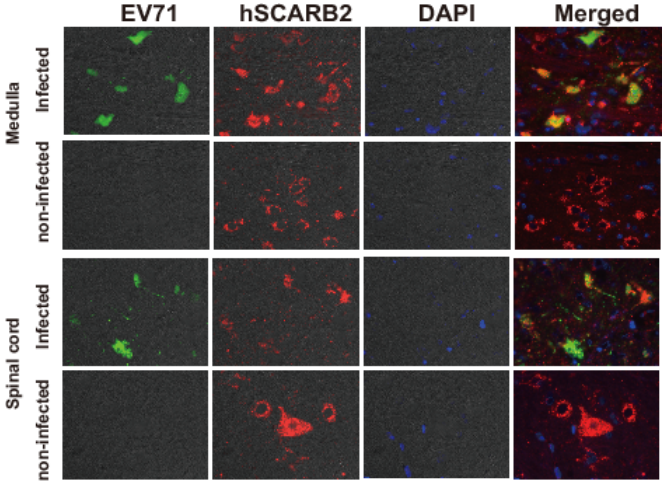

Fig. 3. EV71 infection in hSCARB2-expressing neurons in Tg mice.

Expression profile of hSCARB2 in human and Tg mouse tissues

We performed western blot analysis of human organ samples using a goat anti-hSCARB2 polyclonal antibody (R&D systems). This antibody detected hSCARB2 in western blots of human RD cells and cross-reacted weakly with mouse Scarb2 in mouse L929 cells (31). hSCARB2 signals with apparent molecular weights ranging from 66 to 97 kDa were detected in the western blots of all tested human tissues (Fig. 1A), suggesting that hSCARB2 was expressed in all tissues. Western blot analysis showed marked expression of hSCARB2 in all tested organs of the Tg mouse (Fig. 1B). Together, these data suggest that the human transgene was expressed in all organs of the Tg mouse.

We also examined hSCARB2 expression by immunohistochemistry (IHC). The antibody used for western blotting did not discriminate between endogenous mouse Scarb2 and hSCARB2 in paraffin sections. We therefore used a different anti-hSCARB2 antibody (Sigma) that does not cross-react with mouse Scarb2 in paraffin sections (Fig. 1C). These two antibodies produced indistinguishable staining profiles in human tissues (Fig. S2A). When this antibody was used for IHC, SCARB2 expression was observed in all human and Tg mouse tissues examined but not in non-Tg mouse tissues. Although the staining intensity of hSCARB2 varied among cell types, importantly, hSCARB2 was clearly detected in most CNS neurons in humans and Tg mice but not in non-Tg mice (Fig. 1C and Fig. S2B). The SCARB2 staining for other CNS cell types, such as glial cells and endothelial cells, was much lower in intensity than in neurons. High levels of hSCARB2 expression were also observed in lung pneumocytes, hepatocytes, renal tubular epithelium, splenic germinal centers and intestinal epithelium (Fig. S2B). Similar expression patterns were observed in hSCARB2-Tg16 and 22 mice (Fig.S3). These observations suggest that the expression profile of hSCARB2, including its cell type specificity, is similar in Tg mice and humans.

Susceptibility of hSCARB2-Tg mice to EV71 infection

The EV71 Isehara/Japan/99 (Isehara) strain causes paralysis and death in wild-type neonatal mice but not in those older than 3 weeks. To assess the SCARB2-dependent susceptibility of the hSCARB2-Tg10 mice to EV71 infection, we first inoculated 3-week-old Tg and non-Tg mice intracerebrally with EV71 at several different doses and observed for development of clinical signs. A number of the Tg mice inoculated with the Isehara strain at doses of 10^2-10^6 $TCID_{50}$ showed ataxia, paralysis or death at day 4 to14 post-infection (Table 1, Fig. S4A). In contrast, no neurological manifestations were observed in non-Tg mice (Table 1). Tg mice older than 6 weeks were also susceptible to EV71 infection and the development of disease was similar to that of 3-week-old mice (Fig. S4B). hSCARB2-Tg10 mice were also inoculated via intravenous, intraperitoneal and intragastric routes. Inoculation with EV71 doses greater than 10^2 and 10^3 $TCID_{50}$ via the intravenous and intraperitoneal routes, respectively, led to the development of neurological symptoms although dose dependency was not clear (Table 1). When Tg mice were inoculated intragastrically with EV71 at a dose of 10^6 or 10^7 $TCID_{50}$ per animal, neurological signs were observed in 1 of 20 mice (Table 1). The other Tg mouse strains, hSCARB2-Tg16, 22 and 49 mice, were also susceptible to EV71 infection (Fig. S4C and D). These results showed that adult Tg mice acquired susceptibility to EV71 through the expression of hSCARB2 and that EV71 is able to disseminate from the peripheral tissues to the CNS.

Next, we inoculated 3-week-old hSCARB2-Tg10 mice intracerebrally with several different strains of EV71 [BrCr/USA/70 (BrCr), SK-EV006/Malaysia/97 (SK-EV006), C7/Japan/97 (C7) strains] and a Coxsackie virus A (CVA) 16 G-10 strain. These virus strains have been shown to use hSCARB2 as receptor (32), and it is known that CVA7, 14 and 16 also cause neurological diseases in humans, albeit infrequently (32, 38-40). Infection with the BrCr, SK-EV006, C7 strains caused ataxia, paralysis or death at day 4 to10 post-infection in some mice at more than 10^6, 10^3 and 10^4 $TCID_{50}$, respectively, but some mice remained resistant to disease even after inoculation with the highest dose (10^6 $TCID_{50}$) (Table 2). Similarly, some of the Tg mice inoculated with CVA16 G-10 strain at more than 10^4 $TCID_{50}$ also showed ataxia, paralysis or death at day 7 to10 post-infection. The severity of the disease caused by these virus strains was similar to that caused by the Isehara strain, but much larger virus doses were required. These results suggest that Tg mice are susceptible to EV71 and related viruses that use SCARB2 as receptor, and that the relative sensitivity to each virus strain was different.

Viral replication sites of EV71 in Tg mice

To identify the viral replication sites in 3-week-old Tg mice, we measured the viral titers in major visceral organs at several time points after intravenous inoculation with EV71. The brains and spinal cords of symptomatic mice had high viral titers at days 5 and 7 post-inoculation. The viral titers from asymptomatic Tg

and non-Tg mice were below detectable levels (Fig. 2A). The viral titers in non-CNS organs were also below detection levels in all animals examined. These results suggest that the CNS is the major replication site for EV71 in hSCARB2-Tg10 mice, while replication in other organs remained limited.

Consistent with the virus isolation results (Fig. 2A), we observed pathological changes in the CNS of mice with clinical signs of infection (Fig. 2B, Fig. S5A and Table S2). For example, we observed cellular damage (such as degeneration, necrosis and neuronophagia) and inflammatory changes (such as gliosis and perivascular cuffing) in the spinal cord, brainstem, hypothalamus, thalamus, cerebellum, cerebrum and dorsal root ganglia. Viral antigens were also detected in the affected neurons in these CNS regions (Fig. 2B, Fig. S5A and Table S2), whereas other non-neuronal cell types were negative for viral antigens. We did not detect antigen-positive cells or pathological changes, such as inflammation and pulmonary edema, in regions outside the CNS in any of the mice (Table S2). None of the mice inoculated with EV71 demonstrated cutaneous lesions, regardless of inoculation route. Pathological changes and EV71 antigens in the neurons were also detected in hSCARB2-Tg16, 22 and 49 mice (Fig. S5B).

To confirm that EV71 infection in the neurons of Tg mice was dependent on hSCARB2 expression, we performed double immunofluorescence staining for hSCARB2 and viral antigen. In the medulla oblongata and spinal cord, all viral antigen-positive neurons expressed hSCARB2 (Fig. 3). These data suggest that the expression of hSCARB2 in neurons conferred susceptibility to EV71 infection and led to the neurological symptoms observed in the Tg mice.

Viral replication sites in neonatal Tg mice were also examined by subcutaneous inoculation of 1-day-old non-Tg and Tg mice with the Isehara strain. As expected, infection with the Isehara strain caused paralysis in both non-Tg and Tg mice (Table S3). Viral antigens were detected in the CNS and skeletal muscle of both non-Tg and Tg mice (Table S3). Interestingly, EV71 antigens were also observed in the lungs, in some oral mucosal epithelium cells in the lip and a few skin epidermal cells on terminal parts of limbs, but only in Tg mice (Fig. S5C, Table S3). Viral antigens were not detected in the skin of the trunk. These results suggested that the replication of EV71 in these sites occurred in a SCARB2-dependent manner and that EV71 displays tropism to these cells in neonatal mice.

DISCUSSION

Here, we demonstrated that the exogenous expression of hSCARB2 in mice was sufficient to confer susceptibility to EV71 infection and subsequent development of neuropathogenesis, which suggests that hSCARB2 also functions as a cellular receptor for EV71 infection *in vivo*. EV71 can cause different neurological manifestations in humans such as encephalomyelitis, polio-like flaccid paralysis and meningitis. Although a certain manifestation can be prevalent during a given outbreak, various manifestations can be combined in a patient or different patients in the same outbreak may manifest differently (4, 7, 41-44). In spite of these variations, inflammation and EV71 antigens have been invariably detected in the brainstem, spinal cord, hypothalamus and cerebellar dentate nuclei in fatal human encephalomyelitis (5, 6), suggesting that EV71 has tropism to neurons found therein. In the cynomolgus monkey model, neurological manifestations were observed following intravenous and intraspinal EV71 inoculation ($10^{5.5}$-10^{6} $TCID_{50}$) (14, 15). Histological and viral examinations confirmed viral replication in the spinal cord, brainstem, cerebellar dentate nuclei and cerebrum. Quantitative scoring of these lesions showed that the major foci of replication included the brainstem and dentate nuclei. In comparison, hSCARB2-Tg10 mice infected with EV71 via the intracerebral, intravenous, intraperitoneal or intragastric routes demonstrated paralysis and ataxia, and severe lesions and/or EV71 antigens were observed in the brainstem, spinal cord, hypothalamus, thalamus, cerebellar dentate nuclei and Purkinje layer in most animals (Fig. 2B, Fig. S5A, and Table S2). These results indicate that the spinal cord, brainstem and cerebellar dentate nuclei in this Tg mouse model,were most severely impacted by EV71 infection regardless of the inoculation route. Our findings highlighted the similarities in EV71 neurotropism observed in humans, monkeys and Tg mice. Nonetheless, there were some differences between the Tg mice and humans. Compared to humans, Tg mice were less susceptible to oral infection. Adult Tg mice did not display the typical cutaneous lesions found in human HFMD. Pulmonary edema, which has been reported to be one of the most severe clinical outcomes of human EV71 infection, was not observed in the Tg mouse model. The reasons for these differences remain to be clarified.

In several laboratories, neonatal mice have been used as models for studying EV71 pathogenesis and for the development of vaccines and antiviral drugs(17, 18, 45-47). However, EV71 infection in the neonatal mouse model is significantly different from that in humans as the major viral replication sites in the mouse system include muscle and adipose tissues. EV71 infection in wild-type neonatal mice may be mediated by unknown molecule(s), and increased viral pathogenicity in neonatal mice may have resulted from adaptation of the virus to these molecules acting as receptors. It is possible to avoid this bias by using Tg mice that are more than three weeks old. Our stocks of EV71 BrCr and C7 strains were not pathogenic to neonatal mice, but were pathogenic to hSCARB2-Tg mice suggesting that the viruses did not need to be adapted to rodents for infection to occur (Table 2). Furthermore, susceptibility was still observed in older mice. These results indicate that the hSCARB2-Tg mouse model can be used to overcome the problems associated with traditional neonatal mouse models.

The results in Tg mice suggested the existence of molecular mechanisms that determine EV71 tropism. Recently, another hSCARB2 Tg mouse model was reported (48) in which hSCARB2 was expressed ubiquitously using the human EF-1α promoter. This Tg mouse was susceptible to EV71 only up to 2 weeks of age and the main viral replication sites were in the muscle and the CNS. Therefore, the pathological features of this Tg mouse model were similar to those of the wild-type neonatal mouse model. In contrast, hSCARB2 expression in our hSCARB2-Tg10 mice older than 3 weeks of age was similar to that in humans (Fig. 1C and Fig. S2B), and the majority of viral replication took place in CNS neurons (Fig. 2B and Fig. S5A). These results suggest that differences in virus susceptibility and tissue tropism may be strongly influenced by the expression pattern of hSCARB2. However, high levels of SCARB2 expression were also observed in many non-neural tissues, such as the lung, liver, kidney and intestine of hSCARB2-Tg10 mice, in which EV71 replication was not observed. Together, these results suggest that accurate hSCARB2 expression is necessary for the acquisition of susceptibility but other, as yet unknown, factors could also contribute to efficient viral replication in non-CNS tissues.

The recent large outbreaks of EV71-related HFMD associated with severe neurological consequences represent a major public health concern, especially in the Asia-Pacific region. It can be speculated that circulating EV71 may further increase in neurovirulence. We tested four strains of EV71 and a CVA16, and found that the Isehara strain was associated with the most severe clinical signs among the strains tested. The BrCr, SK-EV006 and C7 strains and the CVA16 G-10 strain were associated with less severe signs although their virulence levels could not be determined accurately because of the low susceptibility of the mice and poor dose-dependent response (Table 2). The

Isehara strain, which was isolated from a HFMD patient, showed an apparent higher neurovirulence in the Tg mouse compared to the other EV71 strains (BrCr, SK-EV006 and C7) isolated from patients with neurological diseases. The CVA16 G-10 strain showed similar virulence level to BrCr (Table 2). One possible explanation for these paradoxical results could be the genetic changes that may have occurred in these viruses following serial passages in cell cultures after the initial isolation. In addition, severity of the human disease may be influenced by multiple factors including amount of virus ingested, and immunological condition and genetic background of the infected person. The neurovirulence level of each virus strain should be determined experimentally using the same background. The neurovirulence levels of these viruses in the monkey model have not been determined yet. It is important to investigate if there is a correlation between the neurovirulence levels determined using the monkey and the Tg mouse models, and to investigate if the virulence levels determined in these models reflect the virulence levels in humans.

In the process of establishing the PVR-Tg mouse model, an appropriate Tg mouse strain (PVR-Tg21) that showed good sensitivity and clear dose-dependent response was chosen (49, 50). In addition, many other investigations were performed, including correlation of neurovirulence levels of viruses in monkey and Tg mouse models (50, 51), and selection of suitable inoculation routes (52). Consequently, PVR-Tg mice became widely used to determine the neurovirulence levels of attenuated and neurovirulent strains of PV (50, 51, 53-55). Analogous to another PVR-Tg mouse strain that expressed PVR at low levels and therefore did not show good sensitivity or dose-dependent response (49), it should be possible to improve the sensitivity of our hSCARB2-Tg mice by developing a new strain with higher hSCARB2 expression levels. With similar efforts conducted for PVR-Tg mice research, our hSCARB2-Tg mice could be used to experimentally evaluate the neurovirulence of field isolates of EV71 with greater statistical significance in the future.

Materials and Methods

Ethics statements. Experiments using recombinant DNA and pathogens were approved by the Committee for Experiments using Recombinant DNA and Pathogens at the Tokyo Metropolitan Institute of Medical Science. Experiments using mice were approved by the Animal Use and Care Committee and performed in accordance with the Guidelines for the Care and Use of Animals (Tokyo Metropolitan Institute of Medical Science, 2011). All human histological samples used in this study were obtained ethically, and the protocols were approved by the relevant ethics committee of University of Malaya.

Cells and viruses. Human RD and African green monkey Vero cells were cultured in Dulbecco's modified Eagle medium supplemented with 5 % fetal calf serum (FCS), L-glutamine and penicillin-streptomycin solution (5 % FCS-DMEM). The prototype strain of EV71, BrCr (genogroup A), was isolated from a patient with aseptic meningitis in 1970 (1). Two isolates, SK-EV006 (genogroup B) (14) and C7 (genogroup B) (56), were obtained from fatal encephalitis cases in 1997. Isehara (genogroup C) was isolated from a case of HFMD (57). The CVA16 G-10 strain was isolated in South Africa (58). We propagated these strains in RD cells.

Virus purification. RD cells were infected with EV71 and CVA G-10 at an MOI of 0.01. The cells and media were frozen at 48 h post-infection. After thawing, the cell debris were removed by centrifugation at 10,000 × g for 20 min at room temperature. Subsequently, 100 mM NaCl, 2 mM EDTA, and 1 % sarkosyl was added to the supernatant, and the supernatant was centrifuged at 14,000 × g for 2.5 h at room temperature. The pellet was resuspended in PBS and then centrifuged through 30% sucrose at 14,000 × g overnight at room temperature. The viral pellet was suspended in 5 % FCS-DMEM.

Virus titration. The viral titers of stock viruses and infected mouse tissues were measured with a microtitration assay using Vero cells as previously described (28).

Mice. To generate Tg mice expressing hSCARB2, two BACs carrying *hSCARB2* genes, RP11-54D17 and RP11-628A4, were purchased from the Children's Hospital Oakland Research Institute BACPAC Resources Center. The BAC clones were purified using a Large-Construct Kit (Qiagen) according to the manufacturer's instructions and suspended in TE buffer (10 mM Tris-HCl, 0.1 mM EDTA, pH 7.5). The purified BAC clones were microinjected into the pronuclei of fertilized mouse eggs (ARK Resource) and then transplanted into pseudo-pregnant CD1 (ICR) mice (Charles River). The resulting mice were screened by PCR analysis using PCR primer sets (Table S1) for the *hSCARB2* gene and genomic DNA extracted from tail biopsies as a template.

Western blot. To investigate the expression of SCARB2 in human tissues, we used a ready-for-use western blot system with human tissue lysates (INSTA-Blot; Imgenex). To prepare the mouse organ protein samples, tissues (100 mg) were homogenized in 1 ml PBS containing a protease inhibitor cocktail (Complete Mini; Roche) with a Polytron homogenizer. The protein concentrations in the samples were determined using a DC protein assay kit (Bio-Rad). The homogenates (5 µg of protein equivalents) were subjected to SDS-PAGE on 12 % gels (Bio-Rad), followed by transfer to the PVDF membrane (Millipore). After blocking, the membranes were incubated for 1 h with a goat anti-human SCARB2 antibody (R&D systems), followed by incubation with an anti-goat horseradish peroxidase (HRP)-conjugated antibody (Jackson ImmunoResearch) and SuperSignal West Pico Chemiluminescent Substrate (Thermo Scientific).

Infection of EV71 in mice. Mice (3-week-old or adults) were inoculated with the viruses at the indicated doses and routes and were observed for clinical signs (Table 1, 2 and Table S2). To evaluate the pathogenesis of EV71 infection in neonatal mice, 1-day-old non-Tg or Tg10 mice were inoculated subcutaneously with EV71 (Fig. S5C and Table S3). To determine the viral titers in mouse tissues, 3-week-old mice were inoculated intravenously with the Isehara strain at a dose of 1×10^6 $TCID_{50}$. The infected mice were sacrificed at the appropriate time post-inoculation. Blood was collected from the heart, and the tissues were removed, frozen at -80°C, thawed and then homogenized in minimal essential medium containing 5 % FCS. After centrifugation for 10 min at 3,000 × *g*, the viral titer of the supernatant was determined in $TCID_{50}$ per gram tissues. Mice were fixed with formalin-buffered saline by perfusion. The removed organs were subjected to IHC.

IHC. Antigen retrieval of formalin-fixed human tissue sections was performed using a rice cooker (30 min, 96-98°C, citrate buffer). Antigen retrieval of formalin-fixed mouse tissue sections was performed by autoclaving at 121°C for 10 min in a retrieval solution of pH 6.0 (Nichirei, Japan) for the detection of viral antigens and a retrieval solution of pH 9.0 (Nichirei, Japan) for the detection of SCARB2 expression. SCARB2 and EV71-antigens were detected in a standard immunoperoxidase procedure using a rabbit anti-human SCARB2 antibody (SIGMA) and anti-EV71 antibody (14), respectively.

Double immunofluorescence staining. Paraffin-embedded sections were stained to evaluate the expression of SCARB2 in virus antigen-positive cells. Following the retrieval reaction by autoclaving in a retrieval solution at pH 9.0, a goat anti-SCARB2 antibody (R&D) and rabbit anti-EV71 antibody were incubated overnight at 4°C. EV71 and SCARB2 were detected following incubation with Alexa Fluor 488 goat anti-rabbit IgG or Alexa Fluor 568 goat anti-mouse IgG (Molecular Probes, Eugene, OR) for 60 min at 37°C, respectively. The sections were mounted in SlowFade Gold antifade reagent containing DAPI (Molecular Probes), and images were captured using a fluorescence microscope (IX71; Olympus, Tokyo, Japan) equipped with a Hamamatsu high-resolution digital B/W CCD camera (ORCA2; Hamamatsu Photonics, Hamamatsu, Japan).

ACKNOWLEDGMENTS.

We thank H. Shimizu for helpful discussions and critical review of the manuscript. We also thank A. Ohkubo, Y. Ichinokawa, A. Harashima, and M. Fujino for excellent technical assistance. This work was supported by JSPS KAKENHI Grant Number 23390116 and 23790518, MEXT KAKENHI Grant Number 24115006 and by a Grant-in-Aid for Research on Emerging and Re-emerging Infectious Diseases from the Ministry of Health, Labor and Welfare of Japan. This study was also partly supported by the HIR grant (UM.C/625/1/HIR/MOHE/MED/06) from the University of Malaya, Malaysia.

1. Schmidt NJ, Lennette EH, & Ho HH (1974) An apparently new enterovirus isolated from patients with disease of the central nervous system. *J Infect Dis* 129(3):304-309.
2. Pallansch M & Roos R (2007) Enteroviruses: Polioviruses, Coxsackieviruses, Echoviruses, and Newer Enteroviruses. *Fields Virology*, eds Knipe DM, Howley PM, D. E. Griffin, Lamb RA, Martin MA, Roizman B, & Straus SE (Lippincott Williams & Wilkins, Philadelphia), 5th edition Ed Vol 1, pp 839-893.
3. Ho M, *et al.* (1999) An epidemic of enterovirus 71 infection in Taiwan. Taiwan Enterovirus Epidemic Working Group. *N Engl J Med* 341(13):929-935.
4. Huang CC, *et al.* (1999) Neurologic complications in children with enterovirus 71 infection. *N Engl J Med* 341(13):936-942.
5. Wong KT, *et al.* (2012) Enterovirus 71 encephalomyelitis and Japanese encephalitis can be distinguished by topographic distribution of inflammation and specific intraneuronal detection of viral antigen and RNA. *Neuropathol Appl Neurobiol* 38(5):443-453.
6. Wong KT, *et al.* (2008) The distribution of inflammation and virus in human enterovirus 71 encephalomyelitis suggests possible viral spread by neural pathways. *J Neuropathol Exp Neurol* 67(2):162-169.
7. Shindarov LM, *et al.* (1979) Epidemiological, clinical, and pathomorphological characteristics of epidemic poliomyelitis-like disease caused by enterovirus 71. *J Hyg Epidemiol Microbiol Immunol* 23(3):284-295.
8. Nagy G, Takatsy S, Kukan E, Mihaly I, & Domok I (1982) Virological diagnosis of enterovirus type 71 infections: experiences gained during an epidemic of acute CNS diseases in Hungary in 1978. *Arch Virol* 71(3):217-227.

9. AbuBakar S, *et al.* (1999) Identification of enterovirus 71 isolates from an outbreak of hand, foot and mouth disease (HFMD) with fatal cases of encephalomyelitis in Malaysia. *Virus Res* 61(1):1-9.
10. Wang Y, *et al.* (2011) Hand, foot, and mouth disease in China: patterns of spread and transmissibility. *Epidemiology* 22(6):781-792.
11. Hashimoto I, Hagiwara A, & Kodama H (1978) Neurovirulence in cynomolgus monkeys of enterovirus 71 isolated from a patient with hand, foot and mouth disease. *Arch Virol* 56(3):257-261.
12. Hashimoto I & Hagiwara A (1982) Studies on the pathogenesis of and propagation of enterovirus 71 in Poliomyelitis-like disease in monkeys. *Acta Neuropathol* 58(2):125-132.
13. Hashimoto I & Hagiwara A (1982) Pathogenicity of a poliomyelitis-like disease in monkeys infected orally with enterovirus 71: a model for human infection. *Neuropathol Appl Neurobiol* 8(2):149-156.
14. Nagata N, *et al.* (2002) Pyramidal and extrapyramidal involvement in experimental infection of cynomolgus monkeys with enterovirus 71. *J Med Virol* 67(2):207-216.
15. Nagata N, *et al.* (2004) Differential localization of neurons susceptible to enterovirus 71 and poliovirus type 1 in the central nervous system of cynomolgus monkeys after intravenous inoculation. *J Gen Virol* 85(Pt 10):2981-2989.
16. Chumakov M, *et al.* (1979) Enterovirus 71 isolated from cases of epidemic poliomyelitis-like disease in Bulgaria. *Arch Virol* 60(3-4):329-340.
17. Chen YC, *et al.* (2004) A murine oral enterovirus 71 infection model with central nervous system involvement. *J Gen Virol* 85(Pt 1):69-77.
18. Wang YF, *et al.* (2004) A mouse-adapted enterovirus 71 strain causes neurological disease in mice after oral infection. *J Virol* 78(15):7916-7924.
19. Wang W, *et al.* (2011) A mouse muscle-adapted enterovirus 71 strain with increased virulence in mice. *Microbes Infect* 13(10):862-870.
20. Khong WX, *et al.* (2012) A non-mouse-adapted enterovirus 71 (EV71) strain exhibits neurotropism, causing neurological manifestations in a novel mouse model of EV71 infection. *J Virol* 86(4):2121-2131.
21. Bergelson JM (2010) Receptors. *The Picornaviruses*, eds Ehrenfeld E, Domingo E, & Roos RP (ASM Press, Washington, DC), pp 73-86.
22. Ren RB, Costantini F, Gorgacz EJ, Lee JJ, & Racaniello VR (1990) Transgenic mice expressing a human poliovirus receptor: a new model for poliomyelitis. *Cell* 63(2):353-362.
23. Koike S, *et al.* (1991) Transgenic mice susceptible to poliovirus. *Proc Natl Acad Sci U S A* 88(3):951-955.
24. Bartlett NW, *et al.* (2008) Mouse models of rhinovirus-induced disease and exacerbation of allergic airway inflammation. *Nat Med* 14(2):199-204.
25. Yang B, Chuang H, & Yang KD (2009) Sialylated glycans as receptor and inhibitor of enterovirus 71 infection to DLD-1 intestinal cells. *Virol J* 6:141.
26. Yang SL, Chou YT, Wu CN, & Ho MS (2011) Annexin II binds to capsid protein VP1 of enterovirus 71 and enhances viral infectivity. *J Virol* 85(22):11809-11820.
27. Nishimura Y, *et al.* (2009) Human P-selectin glycoprotein ligand-1 is a functional receptor for enterovirus 71. *Nat Med* 15(7):794-797.
28. Yamayoshi S, *et al.* (2009) Scavenger receptor B2 is a cellular receptor for enterovirus 71. *Nat Med* 15(7):798-801.
29. Kuronita T, *et al.* (2002) A role for the lysosomal membrane protein LGP85 in the biogenesis and maintenance of endosomal and lysosomal morphology. *J Cell Sci* 115(Pt 21):4117-4131.
30. Reczek D, *et al.* (2007) LIMP-2 is a receptor for lysosomal mannose-6-phosphate-independent targeting of beta-glucocerebrosidase. *Cell* 131(4):770-783.
31. Yamayoshi S & Koike S (2011) Identification of a human SCARB2 region that is important for enterovirus 71 binding and infection. *J Virol* 85(10):4937-4946.
32. Yamayoshi S, *et al.* (2012) Human SCARB2-dependent infection by coxsackievirus A7, A14, and A16 and enterovirus 71. *J Virol* 86(10):5686-5696.
33. Yamayoshi S, Ohka S, Fujii K, & Koike S (2013) Functional comparison of SCARB2 and PSGL1 as receptors for enterovirus 71. *J Virol* 87(6):3335-3347.
34. Tabuchi N, Akasaki K, Sasaki T, Kanda N, & Tsuji H (1997) Identification and characterization of a major lysosomal membrane glycoprotein, LGP85/LIMP II in mouse liver. *J Biochem* 122(4):756-763.
35. Gamp AC, *et al.* (2003) LIMP-2/LGP85 deficiency causes ureteric pelvic junction obstruction, deafness and peripheral neuropathy in mice. *Hum Mol Genet* 12(6):631-646.
36. Ritsch A, *et al.* (2004) Molecular characterization of rabbit scavenger receptor class B types I and II: portal to central vein gradient of expression in the liver. *J Lipid Res* 45(2):214-222.
37. Liu J, *et al.* (2012) Transgenic expression of human P-selectin glycoprotein ligand-1 is not sufficient for enterovirus 71 infection in mice. *Arch Virol* 157(3):539-543.
38. Ranzenhofer ER, Dizon FC, Lipton MM, & Steigman AJ (1958) Clinical paralytic poliomyelitis due to Coxsackie virus group A, type 7. *N Engl J Med* 259(4):182.
39. Helin I, Widell A, Borulf S, Walder M, & Ulmsten U (1987) Outbreak of coxsackievirus A-14 meningitis among newborns in a maternity hospital ward. *Acta Paediatr Scand* 76(2):234-238.
40. Xu W, *et al.* (2012) Distribution of enteroviruses in hospitalized children with hand, foot and mouth disease and relationship between pathogens and nervous system complications. *Virol J* 9(1):8.
41. Samuda GM, Chang WK, Yeung CY, & Tang PS (1987) Monoplegia caused by Enterovirus 71: an outbreak in Hong Kong. *Pediatr Infect Dis J* 6(2):206-208.
42. Melnick JL (1984) Enterovirus type 71 infections: a varied clinical pattern sometimes mimicking paralytic poliomyelitis. *Rev Infect Dis* 6 Suppl 2:S387-390.
43. Lum LC, *et al.* (1998) Fatal enterovirus 71 encephalomyelitis. *J Pediatr* 133(6):795-798.
44. Wang SM, *et al.* (1999) Clinical spectrum of enterovirus 71 infection in children in southern Taiwan, with an emphasis on neurological complications. *Clin Infect Dis* 29(1):184-190.
45. Dong C, *et al.* (2011) Immunoprotection elicited by an enterovirus type 71 experimental inactivated vaccine in mice and rhesus monkeys. *Vaccine* 29(37):6269-6275.
46. Chang JY, *et al.* (2012) Selection and characterization of vaccine strain for Enterovirus 71 vaccine development. *Vaccine* 30(4):703-711.
47. Ong KC, Devi S, Cardosa MJ, & Wong KT (2010) Formaldehyde-inactivated whole-virus vaccine protects a murine model of enterovirus 71 encephalomyelitis against disease. *J Virol* 84(1):661-665.
48. Lin YW, *et al.* (2013) Human SCARB2 transgenic mice as an infectious animal model for enterovirus 71. *PLoS One* 8(2):e57591.
49. Koike S, *et al.* (1994) Characterization of three different transgenic mouse lines that carry human poliovirus receptor gene--influence of the transgene expression on pathogenesis. *Arch Virol* 139(3-4):351-363.
50. Abe S, *et al.* (1995) Studies on neurovirulence in poliovirus-sensitive transgenic mice and cynomolgus monkeys for the different temperature-sensitive viruses derived from the Sabin type 3 virus. *Virology* 210(1):160-166.
51. Horie H, *et al.* (1994) Transgenic mice carrying the human poliovirus receptor: new animal models for study of poliovirus neurovirulence. *J Virol* 68(2):681-688.
52. Abe S, *et al.* (1995) Neurovirulence test for oral live poliovaccines using poliovirus-sensitive transgenic mice. *Virology* 206(2):1075-1083.
53. Dragunsky E, *et al.* (2003) Transgenic mice as an alternative to monkeys for neurovirulence testing of live oral poliovirus vaccine: validation by a WHO collaborative study. *Bull World Health Organ* 81(4):251-260.
54. Kew O, *et al.* (2002) Outbreak of poliomyelitis in Hispaniola associated with circulating type 1 vaccine-derived poliovirus. *Science* 296(5566):356-359.
55. Jegouic S, *et al.* (2009) Recombination between polioviruses and co-circulating Coxsackie A viruses: role in the emergence of pathogenic vaccine-derived polioviruses. *PLoS Pathog* 5(5):e1000412.
56. Shimizu H, *et al.* (1999) Enterovirus 71 from fatal and nonfatal cases of hand, foot and mouth disease epidemics in Malaysia, Japan and Taiwan in 1997-1998. *Jpn J Infect Dis* 52(1):12-15.
57. Shimizu H, *et al.* (2004) Molecular epidemiology of enterovirus 71 infection in the Western Pacific Region. *Pediatr Int* 46(2):231-235.
58. Sickles GM, Mutterer M, Feorino P, & Plager H (1955) Recently classified types of Coxsackie virus, group A; behavior in tissue culture. *Proc Soc Exp Biol Med* 90(2):529-531.

FIGURE LEGENDS

Fig. 1. Expression profiles of hSCARB2 in human and hSCARB2-Tg10 mouse tissues. (A) Expression of hSCARB2 in various human tissues detected using an anti-hSCARB2 antibody. (B) Expression of hSCARB2 in various tissues in Tg and non-Tg mice. Tissues were homogenized and subjected to SDS-PAGE, and hSCARB2 was detected using an anti-hSCARB2 antibody. Arrowheads indicate the positions of hSCARB2 and mScarb2. Asterisks indicate non-specific bands. (C) Immunohistochemical analysis of hSCARB2 expression in human, Tg, and non-Tg mouse CNS tissues stained with an anti-human SCARB2 antibody (brown) and counterstained with hematoxylin. Scale bars represent 50 μm and 100 μm in human and mouse tissue images, respectively.

Fig. 2. Replication of EV71 in the CNS of hSCARB2-Tg10 mice. (A) Viral titers in the brain and spinal cord. After intravenous inoculation of the EV71 Isehara strain at a dose of 1×10^6 $TCID_{50}$ in 3-week-old animals (non-Tg; n=4 in each time point, Tg; n=4 at day 1 and day 3, n=6 at day 5, n=5 at day 7), the mice were euthanized at the indicated times, and the tissues were collected and viral titers measured using the microtiter method. The open and closed circles show the viral titers in individual non-Tg and Tg mice, respectively. The viral titer detection limit is less than 10^3 $TCID_{50}$/g (B) Histopathological changes and viral antigen expression in the CNS of 3-week-old Tg mice inoculated intravenously with the EV71 Isehara strain (shown in Table 1 and Table S2). The pons, medulla, lumbar spinal cord, and cerebellar nuclei are shown (upper panel, H&E staining; lower panel, immunohistochemistry). Open arrowheads, closed arrowheads, and asterisks indicate degenerated neurons, neuronophagia, and gliosis, respectively.

Fig. 3. EV71 infection in hSCARB2-expressing neurons in Tg mice. The medulla and spinal cord sections from a Tg mouse showing neurological signs (listed in Table S2) were double-stained with an anti-EV71 antibody (green) and anti-hSCARB2 antibody (red). Nuclei were stained with DAPI (blue).

==EndOfDocument==

Please review all the figures in this paginated PDF and check if the figure size is appropriate to allow reading of the text in the figure.

If readability needs to be improved then resize the figure again in 'Figure sizing' interface of Article Sizing Tool.